International Journal of Basic and Applied Sciences, 14 (8) (2025) 52-62

International Journal of Basic and Applied Sciences

Website: www.sciencepubco.com/index.php/IJBAS
https://doi.org/10.14419/gyyv8s34
Research paper

Enhancing Convective Heat Transfer with Bisectional Passive Flow Divider Inserts

Suryaji S. Kale [1] *, Sanjaykumar S. Gawade [2]

[1] Mechanical Engineering Department, Department of Technology, Shivaji University, Kolhapur, Maharashtra 416004, India
[2] Mechanical Engineering Department, Rajarambapu Institute of Technology, Rajaramnagar, Sakharale, Affiliated to Shivaji University, Kolhapur, Uran Islampur, Maharashtra, 415414, India
**Corresponding author E-mail: kalesss@gmail.com*

Received: May 25, 2025, Accepted: July 2, 2025, Published: December 4, 2025

Abstract

The high rate at which conventional energy sources are being exhausted has increased the world's attention on the effective use and management of the available energy. Heat exchangers are very important parts of thermal systems, and they are used to transfer the heat energy between two or more fluids. Their thermal performance should be enhanced to increase the overall energy efficiency. This can be done by several heat transfer augmentation methods, which are broadly divided into active, passive, and hybrid methods. Passive techniques are especially appealing among them because they are simple and do not require external energy.
The paper investigates the use of flow divider-type inserts as a passive method of improving heat transfer in a circular tube heat exchanger. The inserts used were 90°, 60°, 45° and 30° twist angle inserts at a Reynolds number range of 7000 to 21000. The experimental results showed that the Nusselt number increased with the Reynolds number, showing that convective heat transfer was improved. Nevertheless, the Thermal Enhancement Factor (ψ) and Friction Factor (f) exhibited a decreasing trend with the Reynolds number.
The insert with 45° twist angle was the most successful in overall performance of all the tested configurations. It produced the best Thermal Enhancement Factor (ψ) and Overall Performance Criteria (η) and was an effective compromise between the heat transfer enhancement and the pressure drop. In particular, the 45° insert showed up to 1.99 times better Nusselt number (Nu), 2.21 times higher heat transfer coefficient (h), 1.7 times higher thermal enhancement factor (ψ), and an Overall Performance Criteria (η) of 1.22 than a plain tube. Conversely, the 30° twist angle, despite enhancing heat transfer, had a very high friction factor that resulted in increased pressure losses and low flow efficiency.

Keywords: *Heat Transfer Enhancement; Inserts; Flow Divider Type; Reynolds Number; Bisectional Inserts.*

1. Introduction

This is one of the basic principles in the field of thermal engineering that can be used for a variety of industrial and engineering applications, such as heat exchangers, cooling technologies, and many more for thermal management systems. Its efficiency decides the entire performance and reliability of these systems, and therefore, people are always seeking ways or methods to accelerate these heat-exchange processes involved. Improvement in convective heat transfer has always been one of the issues of concern with respect to the research priorities of thermal engineering. Among all those techniques which come into play, strategic integration of flow divider inserts promises the most. Inserts are passive in nature, where flow dynamics may be modified, causing disruption to thermal boundary layers, and optimizing friction interactions within the flow field to provide superior heat transfer performance.
Flow dividers are innovative inserts in the flow path of the working fluid in a heat exchange system. These components can induce turbulence, promote mixing of fluids, and disrupt the thermal boundary layer, which in turn can result in a dramatic increase in the heat transfer rates. The focus of this research is on mechanisms by which such inserts affect the fluid flow and thermal performance. It assesses their impacts on convective heat transfer but attempts to look for means to optimize designs and integrate them in an appropriate manner within the thermal system.
This work's experimental apparatus was designed to evaluate performance under a wide range of conditions of flow divider inserts. Parameters that were set in place include the geometric configuration of the insert, flow rate, Reynolds numbers, and working conditions. Forced convection heat transfer and pressure drop characteristics with bisectional passive inserts are the main objective of the research. These inserts are created to maximize heat transfer efficiency but minimize the detrimental effects of increased pressure drop, which provides a balanced approach to thermal optimization.

A comprehensive literature review demonstrates a long interest in enhancing convective heat transfer through different methods. Kumar and Jhinge [18], for example, study the use of segmental baffles in STHE for various geometries and values of Reynolds numbers.
They conclude that the baffle design plays an important role in enhancing heat transfer rates. Another study, carried out by Bichkar et al. [8], was numerical simulations of the effect of helical baffles to establish the impact on thermal efficiency and fluid turbulence.
Ali et al. [10] were concerned with the geometric parameters such as tube length and shell diameter, which had an effect on pressure drop and heat transfer coefficients. This paper was useful for optimizing pitch arrangement for better thermal performance. Joemer et al. [5] applied numerical methods to optimize baffle cut and angle arrangements, and Son and Shin [15] looked into spiral baffles as a potential way of enhancing fluid interaction with the inner shell surface.
The work of Petrik and Gabor [16] is significant for its statistical and simulation-based analysis of horizontal baffles, where the efficiency of such designs is identified under various conditions. Edward and Volker [2] have presented a detailed study on pressure drop in heat exchangers with segmental baffles, including correction factors to bridge experimental and theoretical discrepancies. Further extending the above analysis, Gu et al. [8] considered trapezoidal baffled heat exchangers to obtain substantial improvements in heat transfer coefficients, low pressure drops and better thermal performance factors.
Akpabio et al. [9] examined the influence of the baffle spacing on the overall heat transfer coefficients and obtained some optimum configurations in terms of balanced performance with pressure drop. Similarly, Irshad et al. [20] compared numerical results with experimental data by validating the performance of different orientations and assemblies of baffle systems. Menni et al. [12] introduced W-shaped baffle vortex generators into STHEs to achieve remarkable enhancement in thermal efficiency.
Marzouk et al. [28] proposed an innovative method of air injections with inserts for STHE. The method injected air into sections of tubes that were provided with circular rod inserts, and the results obtained higher heat transfer rates while keeping relatively small pressure drops. Mohammad et al. [17] presented investigations on modified baffle configurations affecting heat transfer performance, wherein it was seen that proper positioning of the tubes contributed significantly to enhanced thermal performance. These studies collectively lay down the varied approaches devised for heat transfer optimization in convective contexts-a foundation on which the present study is based.
Some recent works have examined new insert designs for more effective heat transfer. Dagdevir and Ozceyhan [35] experimentally compared plain, perforated, and dimpled twisted tape inserts and found considerable enhancement in heat transfer performance with acceptable pressure drops. Tabatabaeikia et al. [36] discussed different types of inserts like twisted tapes, wire coils, and perforated strips, describing their working mechanism and comparative thermal enhancement effectiveness. Altwieb et al. [37] researched perforated and louvred fin heat exchangers and reported significant improvements in heat transfer as a result of enhanced turbulence and increased surface area. Vaisi et al. [38] analyzed through experiments various types of perforated tube inserts for condensation heat transfer and demonstrated that well-designed perforations can result in significant thermal enhancement.
Recent studies also highlight the dual effect of nanofluids and insert on thermal improvement. Rashidi et al. [39] critically assessed the synergy between nanofluids and different inserts and found improvements in performance but also gaps, including stability problems and non-standardization of experimental procedures. Hamza and Aljabair [40] carried out an experimental study with hybrid nanofluids and twisted tape inserts in heat exchangers, proving that the combination results in significant improvement in the efficiency of heat transfer.
Manglik and Bergles [57] presented a comprehensive study on the thermal and hydraulic performance of twisted-tape inserts in circular tubes, specifically under transition and turbulent flow regimes. They developed generalized correlations for both the Nusselt number and friction factor by considering a wide range of Reynolds numbers, twist ratios, and geometric configurations. Their experimental findings demonstrated that twisted-tape inserts significantly enhance heat transfer due to the strong swirl flow and secondary motion induced by the twist. However, this enhancement was accompanied by an increase in pressure drop, highlighting the need to evaluate the trade-off between heat transfer improvement and pumping power requirements. The correlations proposed by Manglik and Bergles remain widely cited and serve as a foundational reference for passive heat transfer augmentation techniques in heat exchanger design.
Although much work has been done on inserts and their geometries, very few articles are available regarding the application of bisectional passive inserts. These inserts have performed better than non-continuous twisted tapes, hence they are of special interest in this work.
Thus, the experimental method for testing these inserts under various differential flows was envisioned by the need to explore a range of Reynolds numbers that characterized such differences in flows. Thereby, principal performance parameters to explore included Nusselt Number (Nu), Friction Factor (f), the Thermal Enhancement Factor (ψ), and Overall Performance Criteria (η). This data was fitted into Reynolds number plots in searching for trends, correlations. Although the presence of inserts increases the heat transfer coefficient by disrupting the thermal boundary layer, it also augments the friction factor, demanding more pumping power. This has to be optimized with the geometric design of inserts, so that the effective compromise regarding the efficiency of the heat transfer versus the pressure drop can be struck.
This work comes with significant insight into the design and improvement of heat exchange systems in terms of efficiency. The current study fills the gaps found in the previous literature, and comprehensive experimental data are presented, novel for thermal engineering. The results point to the capability of infrequent bisectional inserts to enhance convective heat transfer, hence providing a promising avenue for designing more efficient and sustainable thermal management solutions for engineering applications. Such a detailed study forms a strong basis for further work, offering practical guidance for developing advanced thermal systems.

2. Theory

Figure 1 is the schematic of methodology and experimental setup. The experimental configuration focuses on a mild steel pipe with an internal diameter of 26 mm, which has been specifically designed to be smooth for air flow. The basic machinery of the flow mechanism is a 2 hp blower, this blows air through the pipe. Flow control valves are installed at the outlet end of the blower so that maximum air can be controlled as required. At the extreme end of the blower outlet, an acrylic venturi meter together with a U-tube manometer measures key parameters such as head, discharge, and air velocity.
The test section is a mild steel pipe of similar dimensions and, as such, enables the observation of airflow and heat transfer characteristics. The heating of the test section is facilitated through a heating coil controlled by a specific regulator, enabling the fine-tuning of the amount of heat being fed into it. This setup ensures adequate heat transfer at the inner wall of the pipe and the moving air. The whole test section is covered with ceramic wool in order to minimize loss of heat to the surroundings. Plastic foam, additional covering above it, acts as extra insulation for thermal purposes.
To get a full thermal analysis, 12 thermocouples are mounted along the test section. These thermocouples give detailed temperature measurements displayed on a temperature indicator board with a 7-segment digital display. Among these readings, T_1 is the air inlet temperature at the test section, and T_{10} is the outlet temperature. The intermediate thermocouples, T_2 through T_9, are spread along the test section length

with a fine thermal profile of air. The temperatures measured are sufficiently accurate for the computation of the rate of heat transfer from the heated pipe to the air.

The experimental procedure starts with airflow analysis through an empty pipe in order to create a baseline. Then, carbon fibre inserts with a width of 25 mm, height of 25 mm, and thickness of 3 mm are introduced into the pipe. These inserts are placed at different angles in order to check the effect on the heat transfer performance. The heat transfer rate from each of these configurations is taken and compared against the baseline obtained. This will, in turn, give a general idea of whether carbon fibre inclusions enhance heat transfer within this pipe.

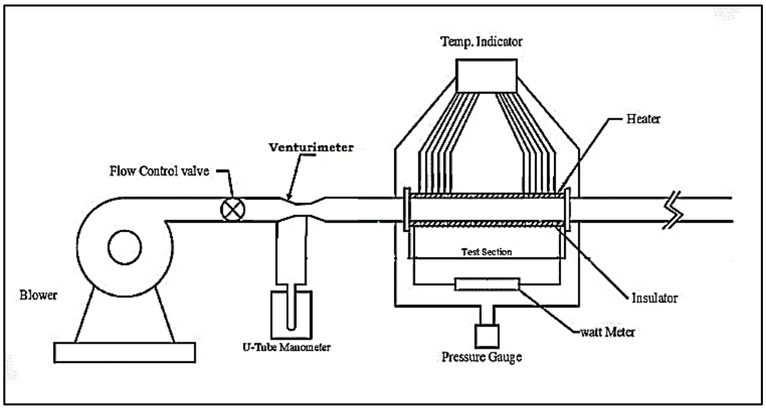

Fig. 1: Illustration of the Experimental Setup.

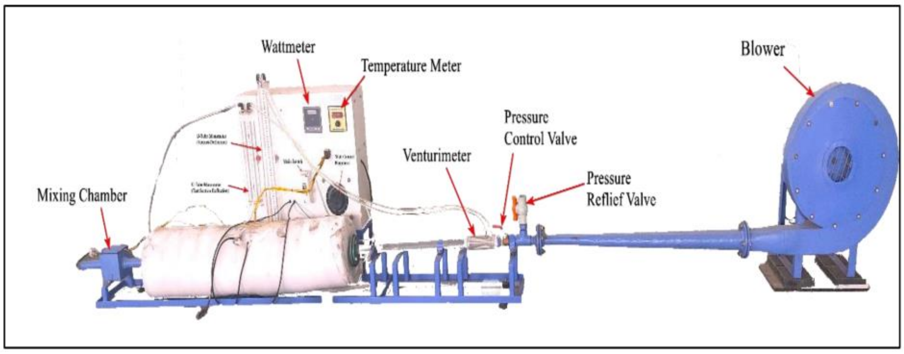

Fig. 1: Photograph of Experimental Set up.

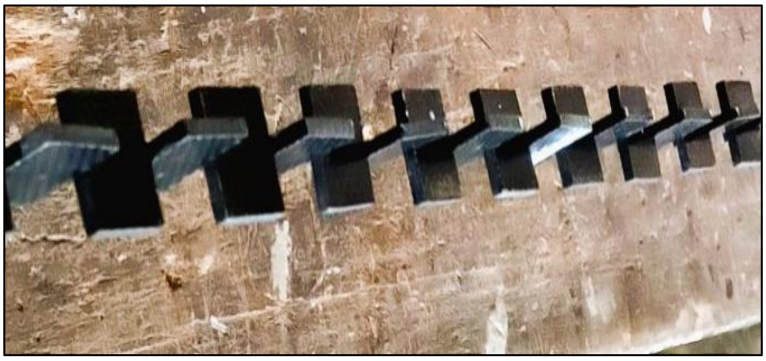

Fig. 3: Continuous Insert at 90° Twist Angle.

Fig. 4: Locating Inserts in the Test Section.

3. Performance Parameters

The following are the performance parameters that determine the performance of the system. The performance evaluation is carried out using a range of equations derived from Fluid Mechanics and Heat Transfer principles. Equation no 1 is taken from the book of Frank M White et al. [33], equations 2,3,4 are taken from the book of Frank P. Incropera et al. [34], equations 5 and 6 are taken from the research paper of P. Nalavade Sandeep et al. [32].

$$Re = \frac{\rho u D}{\mu} \tag{1}$$

In this case, u indicates the average air velocity within the tube, ρ stands for air density measured in kilograms per cubic meter (kg/m^3), D refers to the diameter of the test section pipe in meters (m), and μ represents dynamic viscosity, expressed in Pascal-seconds (Pa·s).
The formula below calculates the total heat transferred to the air:

The *Re* for the airflow in the test section is determined using the following expression:

$$Q = \dot{m} C_P (T_o - T_i) \tag{2}$$

In this case, T_i and T_0 denote the air's inlet and outlet temperatures as it flows through the test section. The symbol ṁ represents the air's mass flow rate in kilograms per second (kg/s), and Cp stands for the specific heat capacity of air, measured in kilojoules per kilogram per kelvin (kJ/kg·K).
The heat transfer coefficient can be calculated using the following expression:

$$Q = h\, A_s (T_w - T_{mb}) \tag{3}$$

The coefficient of heat transfer at the interface is given by h in W/m^2·K.. The area of thermal transfer is given by As in m^2. This expression (3) describes the convective heat transfer rate Q from a surface in terms of the surface area As, the convective heat transfer coefficient h, and the temperature difference between the wall temperature, T_w, and the bulk mean temperature of the fluid T_{mb}. This equation is very important for the study of mechanism of heat transfer in engineering and science contexts.
The Nusselt number *Nu*, and friction factor *f* are the parameters used to characterize the effect of heat transfer and fluid flow, hence illustrating the relationship between these two factors as follows:

$$u = \frac{hD}{k} \tag{4}$$

Nu is the dimensionless number describing the convective heat transfer coefficient in comparison with the conductive heat transfer. The coefficient of heat transfer *h* is measured in watts per square meter per kelvin, W/m^2.K. D is the diameter of the pipe in m. Another important parameter involved in the heat transfer is thermal conductivity of fluid k in watts per meter per kelvin W/m·K

$$f = \frac{\Delta P}{\left(\frac{1}{2}\right)\rho u^2 \left(\frac{1}{d}\right)} \tag{5}$$

Where ΔP represents the pressure difference over the test section length (measured in pascals) and k denotes the thermal conductivity (expressed in watts per meter-kelvin).
Thermal Enhancement factor (ψ) is defined as;

$$\psi = \frac{h}{h_0} \tag{6}$$

Where h = Corvective heat transer coefficient for plain tube fitted with flow divider type insert (W/m^{2}K) and, h_0 = Convective heat transfer coefficient for plain tube (W/m^{2}K). A plain tube is a tube without any insert or an empty tube.
The performance evaluation criteria (η) is calculated as the ratio of the Nusselt number $\left(\frac{Nu}{Nu_0}\right)$ to the corresponding friction factor ratio. $\left(\frac{f}{fo}\right)^{1/3}$ Both were measured under identical blower power conditions.

$$\eta = \frac{\left(\frac{Nu}{Nu_0}\right)}{\left(\frac{f}{f_0}\right)^{\frac{1}{3}}} \tag{7}$$

4. Results and Discussion

Using different graphical representations, analysis is done for the experimental data in several observation parameters, which are recorded for various Reynolds numbers. This investigation addresses the influence of changing the twist angle for a flow divider-type insert on the performance of convective heat transfer.
The findings are that as the Reynolds number increases, the rate of convective heat transfer increases with it. This is because the flow rate has increased, and thus the turbulence in the system increases.
Experimental data were taken at various twist angles, 90°, 60°, 45°, and 30°, for Reynolds numbers between 7000 and 21000. The results were graphically presented in plots of parameters such as the Nusselt number (*Nu*), friction factor (*f*), thermal enhancement factor (ψ), and performance evaluation criteria (η) against the Reynolds number. These plots were used to determine the trends and obtain meaningful conclusions.
Figure 5. Effect of different twist angles in flow divider inserts on the heat transfer coefficient: The graph is a representation of the relationship between twist angle and heat transfer coefficient at different Reynolds numbers. For a higher Reynolds number, the heat transfer

coefficient h increases linearly, which is a reflection of better convective heat transfer at a higher flow rate. Inserts with smaller twist angles of 30° and 45° of twist angle perform better than larger ones, for example, 90°, because of the turbulence developed and better fluid mixing. Coefficient of heat transfer (h) was to be found in the range 1.99 times to 1.3 times, 2.33 times to 1.58 times, 3.48 times to 1.92 times, and 2.38 times to 1.45 times that of the insert without the insert for twist angles of 90°, 60°, 45°, and 30°, respectively.
The absence of an insert results in the lowest h values, emphasizing the effectiveness of these devices in disrupting the boundary layer and promoting heat transfer.

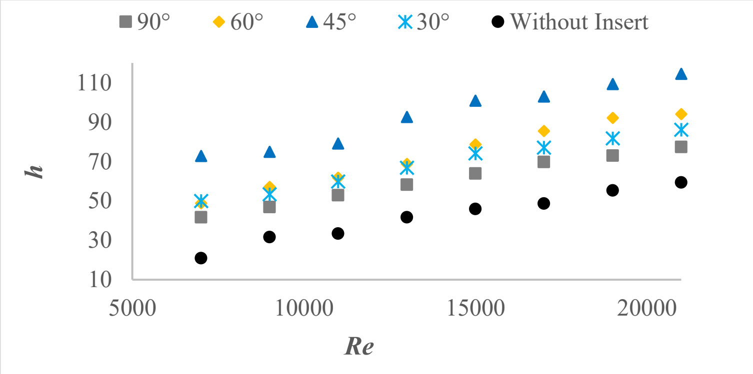

Fig. 5: Effect of Varying the Twist Angle of Flow Divider-Type Inserts on the Heat Transfer Coefficient.

Figure 6 shows how the twist angle of flow divider inserts affects the Nusselt number. The graph highlights the relationship between Reynolds number (*Re*) and Nusselt number (*Nu*) for various twist angles (90°, 60°, 45°, and 30°), along with a baseline case without an insert. The Nusselt number, which reflects the effectiveness of convective heat transfer, consistently rises as *Re* increases for all scenarios. Inserts with smaller twist angles (e.g., 45° and 30°) exhibit superior performance, achieving higher *Nu* values compared to larger twist angles (90° and 60°). The "without insert" case consistently shows the lowest *Nu* values, emphasizing the significant enhancement in convective heat transfer achieved with inserts. Figure 6 highlights the relationship between the Nusselt number (*Nu*) and the Reynolds number (*Re*) for different insert angles (90°, 60°, 45°, 30°), as well as for the baseline scenario without an insert. The Nusselt number serves as an indicator of heat transfer efficiency, while the Reynolds number defines the flow regime. The findings indicate that reducing the twist angle from 90° to 30° leads to a substantial increase in the Nusselt number. Specifically, the Nusselt number is found to be 1.3 to 1.99 times, 1.58 to 2.33 times, 1.75 to 2.98 times, and 1.45 to 2.38 times greater than the no insert results for twist angles of 90°, 60°, 45°, and 30°, respectively, compared to the case without an insert.

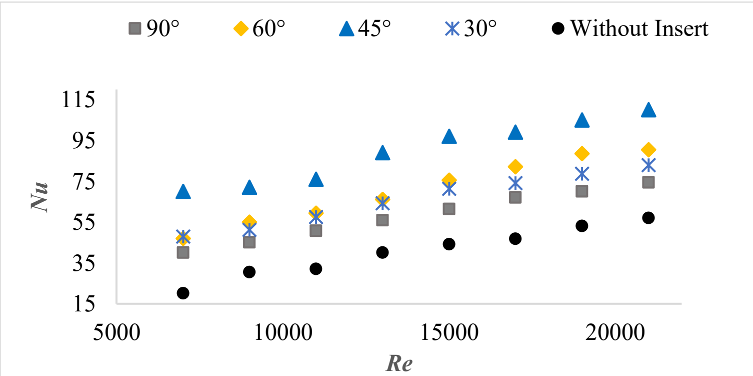

Fig. 6: Effect of Varying the Twist Angle of the Flow Divider Insert on the Nusselt Number.

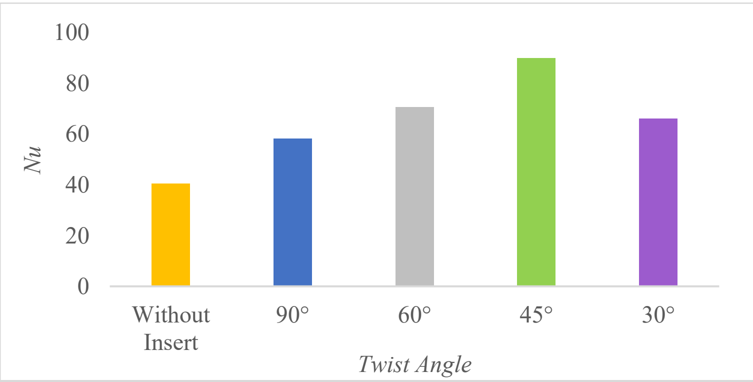

Fig. 7: Average Nusselt Number Comparison Across Various Twist Angle.

The bar graph in Figure 7 shows how the average Nusselt number (*Nu*) changes with different twist angles of a flow divider insert. Among the tested angles, the 45° twist delivers the highest average *Nu*, indicating the most efficient heat transfer.
Figure 8 shows the Influence of the Twist Angle of the Flow Divider Insert on the Friction Factor. This graph illustrates the relationship between the twist angle of a flow divider insert and the friction factor in fluid flow systems. As the twist angle increases from no insert to 90°, the friction factor shows a significant rise, particularly at higher Reynolds numbers. This behavior is primarily due to the increased

turbulence and mixing caused by the insert at higher twist angles (30°, 45°, 60°, and 90°). The friction factor ranges from 0.10 to 0.07 for a 90° angle, 0.28 to 0.18 for a 60° angle, 0.30 to 0.20 for a 45° angle, and 0.37 to 0.30 for a 30° angle. On average, the friction factor for a 45° twist angle is approximately seven times higher than that of a plain tube, which is largely attributed to the obstruction of airflow by the insert. The friction factor experiences an increase of 2.36 to 2.61, 6.52 to 6.5, 6.87 to 7.04, and 8.58 to 10.73 as the twist angle of the insert progresses from no insert to 90°, 60°, 45°, and 30°, respectively. These orientations of the insert and the subsequent flow disturbances result in greater energy dissipation and, therefore, greater frictional losses. These results are very important to optimize the design of the flow divider inserts with reduced energy losses and thus more efficient systems for different values of the Reynolds number.

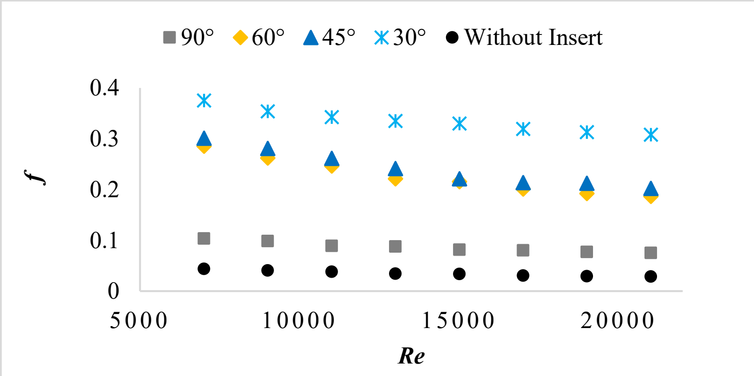

Fig. 8: Effect of Varying the Twist Angle of Flow Divider Inserts on the Friction Factor.

Figure 9 illustrates the effect of the cyclic twist angle of a flow divider insert on the friction factor ratio, f/f_o. The graph demonstrates how varying the twist angle influences frictional behavior within a fluid flow system. As the twist angle increases from a straight flow (no insert) up to 90°, the friction factor ratio generally rises, with the effect becoming more prominent at higher Reynolds numbers.

This upward trend is primarily attributed to enhanced turbulence and intensified mixing triggered by the insert. Twist angles such as 30°, 45°, 60°, and 90° introduce more pronounced disturbances in the flow direction, increasing energy dissipation and, consequently, frictional resistance.

Twisted inserts with a 30º twist angle are widely used to enhance heat transfer in thermal systems. The sharp twist introduces a strong swirling motion in the fluid, which increases turbulence and disrupts the boundary layer near the heated surface. This promotes better mixing of the fluid bringing cooler fluid from the core toward the wall and pushing warmer fluid away, resulting in improved convective heat transfer. Consequently, the Nusselt number, a measure of heat transfer efficiency, increases significantly.

However, this improved thermal performance comes with a trade-off. The tighter twist also increases flow resistance, leading to a higher pressure drop across the system. To maintain the desired flow rate, more pumping power is needed, which increases energy consumption. This added hydraulic penalty must be considered in system design.

To evaluate the balance between thermal gains and energy cost, engineers use the Performance Evaluation Criterion (η). A 30 ° twist angle often offers a good improvement in overall performance, but whether it is the best choice depends on the application's specific heat transfer requirements and energy constraints.

Whereas the 30° twisted insert exhibits a large swirl factor (ψ) and considerable improvement in heat transfer caused by enhanced turbulence and effective boundary layer disruption, its performance is overall restricted by excessive flow resistance. The close twist causes significant secondary flows that enhance mixing and increase the Nusselt number but do so at a considerable cost of pressure drop, thus increasing the pumping power needed. When evaluated using the Performance Evaluation Criterion (η), which optimizes thermal improvement against hydraulic loss, the 30° insert performs worse than the 45° insert. While the 30° insert has better heat transfer, its high friction penalty negates the thermal gain, rendering it less effective in terms of net energy performance. This trade-off also makes it crucial to assess not only the heat transfer potential but also the energy cost involved with it when deciding the best configuration for real-world applications.

The friction factor ratio varied between 2.36 and 2.61, from 6.52 to 6.5, and was found to increase to 8.58 and 10.73 as the cyclic twist angle changed from no insert to 90°, 45°, and 30°, respectively. These details would therefore be quite precious for the intent of optimization for the design flow divider inserts, which should decrease the energy losses due to varying the Reynolds number, which ranged between 7000 and 21000.

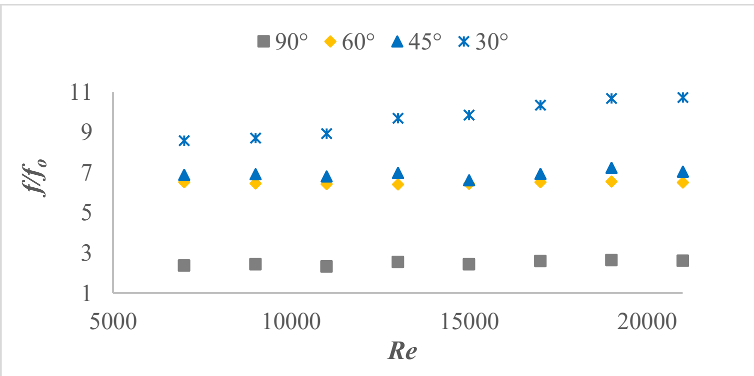

Fig. 9: Effect of Variations in the Cyclic Twist Angle of the Flow Divider-Type Insert on the Friction Factor Ratio (F/F_0).

Figure 10 illustrates how the cyclic twist angle of the flow divider insert affects the thermal enhancement factor (ψ). The graph examines the influence of varying twist angles on the thermal enhancement factor within a fluid flow system. As the cyclic twist angle increases, ranging from no insert to 90°, the thermal enhancement factor tends to rise, particularly at elevated Reynolds numbers.

This enhancement in thermal performance is attributed to the increased turbulence and mixing induced by the insert at larger cyclic angles (30°, 45°, 60°, and 90°). The graph in Figure 10 shows that reducing the twist angle from 90° to 60°, 45°, and 30° results in an increase in the thermal enhancement factor. The thermal enhancement factor shows an increase ranging from 1.28 to 1.43 times for a 90° angle, 1.38 to 1.65 times for 60°, 1.39 to 1.72 times for 45°, and 1.48 to 2.13 times for 30°, compared to a plain tube without an insert. The insert's orientation and the flow disturbances it generates improve heat transfer, thereby enhancing the thermal performance of the system. This information is valuable for optimizing flow divider inserts in applications that require better thermal performance across various Reynolds numbers (7000 to 21000).

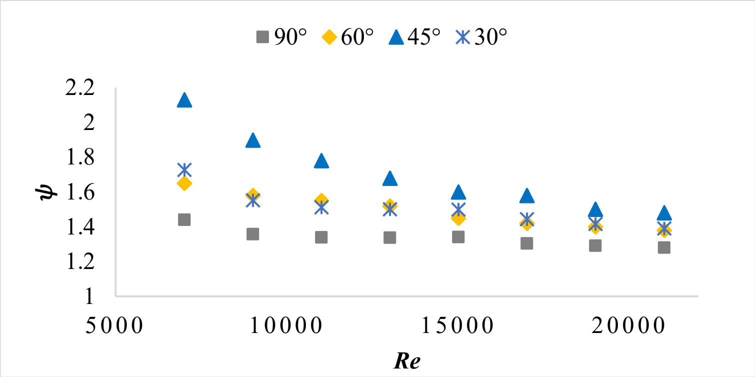

Fig. 10: Effect of Varying the Cyclic Twist Angle of Flow Divider-Type Inserts on the Thermal Enhancement Factor.

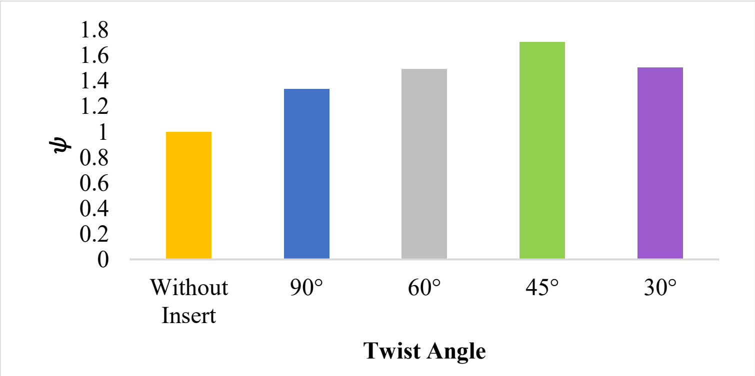

Fig. 11: Average Thermal Enhancement Factor Comparison Across Various Twist Angles.

The graph in Figure 11 presents how the average thermal enhancement factor (ψ) varies with different twist angles of flow divider-type inserts. Without any insert, the enhancement factor is lowest, indicating minimal thermal improvement. As twist angles are introduced, there is a noticeable rise in ψ, with the 45° angle delivering the highest enhancement.

Figure 12. Variation of cyclic twist angle for a flow divider-type insert modifies the Overall Performance Criteria η. The graph shows the effects of the twist angle of the insert on total enhancement in a fluid flow system. Enhancement criteria at different Reynolds numbers typically increase with the increase in the cyclic twist angle from no insert to 90°. Such enhancements are primarily due to increased turbulence and mixing effects developed by the insert at larger angles of 30°, 45°, 60°, and 90°. The general improvement criteria η, which are the observed values, range from 1.49 and 0.94, 1.24 and 0.84, 1.83 and 1, and 0.81 and 0.94 for the twist angles of 90°, 60°, 45°, and 30° compared to the no insert condition, respectively. The flow disruptions created by the insert positioning and its presence contribute significantly to enhancing heat transfer and pressure drop and thus overall system performance. These results will be very helpful for the design optimization of flow divider inserts when applications require the highest overall performance within a Reynolds number range of 7000 to 21000.

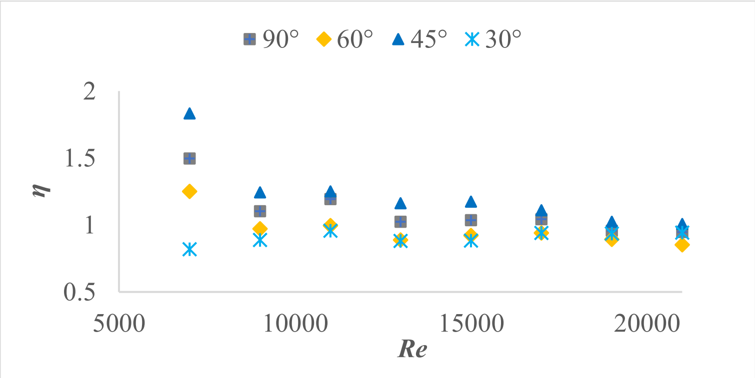

Fig. 12: Effect of Varying the Cyclic Twist Angle of Flow Divider Inserts on the Overall Performance Criteria.

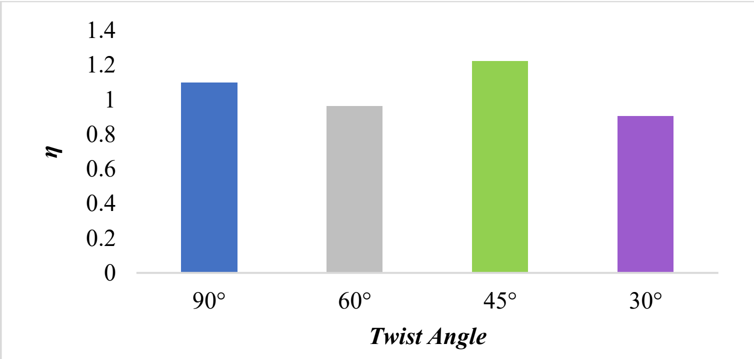

Fig. 13: Average Overall Performance Criteria Comparison Across Various Twist Angles.

The bar graph in Figure 13 illustrates the effect of twist angle on the average Overall Performance Criteria (η) for flow divider inserts. Among the four twist angles evaluated, the 45° insert stands out, showing the highest overall enhancement, which implies an optimal trade-off between improved heat transfer and pressure drop.
Table no. 1 shows key metrics comparison (Nu, f, ψ, η) across twist angles and Reynolds numbers for quick reference.

Table 1: Key Metrics (Nu, f, ψ, η) Across Twist Angles and Reynolds Numbers

Twist Angle	*Re*	*Nu*	*f*	*ψ*	*η*
90°	7000	40.1235	0.10354	1.4394	1.49635
	9000	45.1256	0.0986	1.3565	1.102645
	11000	50.785	0.08902	1.3398	1.193379
	13000	55.9642	0.08771	1.3375	1.022306
	15000	61.4562	0.08164	1.3415	1.034411
	17000	67.1456	0.0801	1.3044	1.042527
	19000	70.1564	0.07739	1.2917	0.95574
	21000	74.4562	0.07502	1.2804	0.946538
60°	7000	46.9542	0.2855	1.65	1.248756
	9000	54.9652	0.2622	1.58	0.96943
	11000	59.4562	0.2466	1.55	0.994809
	13000	66.1234	0.2211	1.52	0.887525
	15000	75.6395	0.2155	1.45	0.921219
	17000	82.2296	0.2011	1.42	0.939376
	19000	88.6596	0.1922	1.4	0.891888
	21000	90.56123	0.1865	1.38	0.849859
45°	7000	47.97	0.3012	1.7266	1.831968
	9000	51.3	0.28123	1.552	1.243071
	11000	57.56	0.26145	1.5123	1.249097
	13000	64.23	0.24123	1.5003	1.16202
	15000	71.3	0.221362	1.4986	1.172339
	17000	74.17	0.2136	1.4442	1.109835
	19000	78.65	0.21236	1.4161	1.022928
	21000	82.91	0.20213	1.3912	1.006084
30°	7000	70.1236	0.37547	2.1301	0.816799
	9000	72.1456	0.3539	1.8973	0.887033
	11000	76.1235	0.34288	1.78	0.955393
	13000	89.1256	0.33507	1.68	0.879766
	15000	97.1235	0.32988	1.6	0.882348
	17000	99.1235	0.31912	1.58	0.939354
	19000	105.1236	0.31318	1.5	0.934318
	21000	110.1235	0.30792	1.48	0.940814

5. Conclusion

This research experimentally examines fluid flow and heat transfer behavior within a circular tube equipped with bisectional passive flow divider turbulators under turbulent conditions. The heat exchanger tube's performance was evaluated using flow divider turbulators with twist angles of 90°, 60°, 45°, and 30°.
These turbulators effectively disturb the boundary layer, leading to enhanced thermal performance. The primary findings of this experimental investigation are as follows:

1) The experimental findings indicate that the Heat Transfer Coefficient (h) increases by factors of 1.99 to 1.3, 2.33 to 1.58, 3.48 to 1.92, and 2.38 to 1.45 when compared to a plain tube, for twist angles of 90°, 60°, 45°, and 30°, respectively.
2) As the twist angle decreases, the flow blockage increases, enhancing fluid mixing and convective heat transfer. The corresponding Nusselt numbers range from 40.12 to 74.45 for 90°, 46.95 to 90.56 for 60°, 70.12 to 110.12 for 45°, and 47.97 to 82.9 for 30°.
3) The Thermal Enhancement Factor (ψ) improves significantly with reduced twist angles. It increases by 1.28 to 1.43 times for 90°, 1.38 to 1.65 times for 60°, 1.48 to 2.13 times for 45°, and 1.39 to 1.72 times for 30°, related to a plain tube.
4) The friction factor (f) is highest at the 30° twist angle due to pronounced flow restriction, ranging from 0.30 to 0.37 across the evaluated angles.
5) The Overall Performance Criteria (η) were observed to range from 1.49 to 0.94, 1.24 to 0.84, 1.83 to 1, and 0.81 to 0.94 for twist angles of 90°, 60°, 45°, and 30°, respectively, compared to the bare tube.

6) The best outcomes were obtained for the 45° twist angle, which showed a 1.99 times increase in Nu, a 2.21 times increase in h, a thermal enhancement factor ψ of 1.7 times, and an Overall Performance Criteria η of 1.22 times compared to the plain tube.

However, the solid flow dividers used in the current setup partially obstruct the flow passage, resulting in increased friction and pumping power. Introducing a sporadic arrangement of inserts or porous flow dividers could optimize heat transfer efficiency while minimizing friction.

Nomenclature

A : The surface area of the experimental test section is expressed in square meters (m^2).
Cp : The specific heat of air at constant pressure, Measured in joules per kelvin (J/K).
D : The internal width of the plain tube, expressed in meters (m).
f : A dimensionless value representing the friction factor.
h : The average coefficient for convective heat transfer, measured in $W/m^2{\cdot}K$.
k : Thermal conductivity, defined as the material's capability to transfer heat, expressed in watts per meter per kelvin (W/m·K)
L : The length of the test section, given in meters (m).
$\dot{m}$: The mass flow rate, representing the quantity of mass passing through per unit of time, is measured in kilograms per second (kg/s).
Nu : Nusselt number, a dimensionless quantity.
P : Insert pitch, measured in meters (m).
P_r The Prandtl number is a dimensionless parameter.
Q : The rate of heat transfer, expressed in watts (W).
R_e The Reynolds number represents a dimensionless value.
S : Space between the two blades of the insert, in meters (m).
T_i : The fluid's starting temperature, measured in degrees Celsius (°C).
T_o : The fluid's final temperature, given in degrees Celsius (°C).
T_w : The wall surface temperature, expressed in degrees Celsius
T_{mb} : The average temperature of the bulk fluid, specified in degrees Celsius (°C).
$\dot{v}$: Volume Flow Rate (m^3/s) - Volume of fluid passing through per unit time, in cubic meters per second.

Greek symbols

ρ : Density (kg/m^3) - Mass per unit volume, measured in kilograms per cubic meter
μ : Dynamic viscosity (Ns/m^2) refers to a fluid's resistance to internal motion, quantified in Newton-seconds per square meter.
ψ : Thermal enhancement factor, TEF - Dimensionless factor representing thermal enhancement.
η : Overall Performance Criteria – Criteria used for performance evaluation.

Subscripts

i : Inlet
o : Outlet
bm: Bulk mean
0 : Plain tube
s : Surface

Author Contribution

The authors confirm their contribution to the paper as follows: Study conception and design: Suryaji S. Kale, Sanjaykumar S. Gawade; Data collection: Suryaji S. Kale; Analysis and interpretation of results: Suryaji S. Kale; Draft manuscript: Suryaji S. Kale; All authors reviewed the results and approved the final version of the manuscript.

Acknowledgement

The author sincerely acknowledges the invaluable support and research facilities provided by Nagesh Karajagi Orchid College of Engineering and Technology, Solapur. Their generous assistance and resources played a crucial role in facilitating the successful completion of this research work.

References

[1] Dwivedi, Abhay Agrawal, Ayush Galphat, Neeraj Sharma, Materials Today, 4th International Conference on Advances in Mechanical Engineering and Nanotechnology Science Direct, Volume 63, 2022, Pages 726-730. https://doi.org/10.1016/j.matpr.2022.05.071.
[2] G. Edward and G. Volker (1997). Pressure drop on the shell side of shell-and-tube heat exchangers with segmental baffles. Chemical Engineering and Processing, Vol 36, , pp. 149-159. https://doi.org/10.1016/S0255-2701(96)04194-3.
[3] Nihat Biçer, Tahsin Engin “, Halit Yas¸ar, Ekrem Büyükkaya, Ahmet Aydın, Adnan Topuz c (2020). Design optimization of a shell-and-tube heat exchanger with novel three-zonal baffle by using CFD and taguchi method. International Journal of Thermal Sciences. https://doi.org/10.1016/j.ijthermalsci.2020.106417.
[4] Kim Leong Liaw, Jundika C. Kurnia, Zulfan A. Putra, Muhammad Aziz, Agus P. Sasmito, Enhanced turbulent convective heat transfer in helical twisted Multilobe tubes, International Journal of Heat and Mass Transfer Volume 202, March 2023, 123687. https://doi.org/10.1016/j.ijheatmasstransfer.2022.123687.
[5] Joemer. C. S, Sijo Thomas, Rakesh. D, Nidheesh. P (2015). Optimization of Shell & Tube Heat Exchanger by Baffle Inclination and Baffle Cut. International Journal of Innovative Research in Science, Engineering and Technology, vol.4.

[6] Emad M.S. El-Saida, M.M. Abou Al-Sood (2019). Shell and tube heat exchanger with new segmental baffles configurations: A comparative experimental investigation. Applied Thermal Engineering. https://doi.org/10.1016/j.applthermaleng.2019.01.039.
[7] Suryaji S. Kale, S. S. Gawade (2022). Heat Transfer Augmentation in Forced Convection with Regularly Spaced Inserts—A Review. Techno-Societal 2022 Proceedings of the 4th International Conference on Advanced Technologies for Societal Applications—Volume 2, Springer.
[8] P. Bichkar, O. Dandgaval, P. Dalvi, R. Godase and T. Dey (2018). Study of Shell and Tube Heat Exchanger with the Effect of Types of Baffles. Procedia Manufacturing, Vol.20, , pp. 195–200. https://doi.org/10.1016/j.promfg.2018.02.028.
[9] Suryaji S. Kale, S. S. Gawade, B. R. Birajdar (2022). Improving Conversion Efficiency of Solar Panel by Cooling System. Techno-Societal 2022 Proceedings of the 4th International Conference on Advanced Technologies for Societal Applications—Volume 2, Springer.
[10] Ali Akbar Abbasian Arania, Reza Moradia (2019). Shell and tube heat exchanger optimization using new baffle and tube configuration. Applied Thermal Engineering. https://doi.org/10.1016/j.applthermaleng.2019.113736.
[11] E. Akpbio, I. Oboh, and E. Aluyor (2009).The effect of Baffles in Shell and Tube Heat exchangers. Advanced Materials Research Vol 62-64, , pp 694-699. https://doi.org/10.4028/www.scientific.net/AMR.62-64.694.
[12] Younes Menni, Ali J. Chamkha, Houari Ameur, Mustafa (2020). Enhancement of the Hydrodynamic Characteristics in Shell-and-Tube Heat Exchangers by Using W-Baffle Vortex Generators. Periodica Polytechnica Mechanical Engineering, 64(3), pp. 212–223. https://doi.org/10.3311/PPme.15493.
[13] Mohammad Fares, Mohammad AL-Mayyahi, Mohammed AL-Saad (2020). Heat transfer analysis of a shell and tube heat exchanger operated with graphene nanofluids. Case Studies in Thermal Engineering. https://doi.org/10.1016/j.csite.2020.100584.
[14] M. Arulprakasajothi, N. Poyyamozhi, A. Saranya, K. Elangovan, Yuvarajan Devarajan, S. Murugapoopathi, Kassian T.T. Amesho, An experimental investigation on winter heat storage in compact salinity gradient solar ponds with silicon dioxide particulates infused paraffin wax, Journal of Energy Storage, Volume 82, 30 March 2024, 110503. https://doi.org/10.1016/j.est.2024.110503.
[15] Y. Son and J. Shin (2001). Performance of a shell and tube heat exchanger with spiral baffles plates. KSME International Journal, Vol.15, , pp 1555-1562. https://doi.org/10.1007/BF03185746.
[16] M. Petrik and G. Szepesi (2018). Shell side CFD analysis of a model shell and tube heat exchanger. Chemical engineering, vol. 70. https://doi.org/10.1002/er.1272.
[17] Philippe Wildi-Tremblay and Louis Gosselin (2007). Minimizing shell-and-tube heat exchanger cost with genetic algorithms and considering maintenance. International Journal of Energy Research. https://doi.org/10.14445/22315381/IJETT-V15P281.
[18] N. Kumar and P. Jhinge (2014). Effect of segmental baffles at different orientation on the performances of single pass shell and tube Heat exchanger. International Journal of engineering trends and technology, vol 15.
[19] Hasanen M. Hussen, Laith Habeeb, Zena K. Kadhim, Heat Transfer Enhancement by Using Twisted Tape in Horizontal and An Inclined Tube, Journal of Mechanical Engineering Research and Developments ISSN: 1024-1752 CODEN: JERDFO Vol. 43, No. 3, pp. 106-124, 2020.
[20] Mohammed Irshad, Mohammed Kaushar, G. Rajmohan (2017). Design and CFD Analysis of Shell and Tube Heat Exchanger. International Journal of Engineering science and computing, Vol. 7.
[21] Manjesh Bandrehalli Chandrashekaraiah, Beemkumar Nagappan, Yuvarajan Devarajan, Hybrid Power Generation: Experimental Investigation of PCM and TEG Integration with Photovoltaic Systems, International Research Journal of Multidisciplinary Technovation, Volume 6, Issue 3, Year 2024. https://doi.org/10.54392/irjmt24317.
[22] Huijun Feng, Lingen Chen, Zhixiang Wu, Zhuojun Xie (2019). Constructal design of a shell-and-tube heat exchanger for organic fluid evaporation process. International Journal of Heat and Mass Transfer. https://doi.org/10.1016/j.ijheatmasstransfer.2018.11.105.
[23] Jothilingam M, Balakrishnan N, Kannan T.K, Yuvarajan Devarajan, Experimental investigation of a solar still system with a preheater and nanophase change materials, Proceedings of the Institution of Mechanical Engineers, Part E: Journal of Process Mechanical Engineering.
[24] G. Xin, Y. Luo, X. Xiong, K. Wang and Y. Wang (2018). Numerical and experimental investigation of the heat exchanger with trapezoidal baffles. International Journal of Heat and Mass Transfer, Vol.127, , pp. 598-606. https://doi.org/10.1016/j.ijheatmasstransfer.2018.07.045.
[25] Ali, M. Kareem, and S. Naji (2018). Performance analysis of shell and tube heat exchanger parametric study. Case studies in thermal engineering, Vol.12, , pp 563-568. https://doi.org/10.1016/j.csite.2018.07.009.
[26] Abhishek Singh, Mohan Gupta, Dharmendra Kumar Tiwari, Rajendra Prasad Verma, Utilization of aluminium helically corrugated twisted tape inserts for heat transfer enhancement of turbulent flow Materials Today, Science Direct, Volume 92, Part 2, 2023, Pages 1623-1628. https://doi.org/10.1016/j.matpr.2023.06.107.
[27] Z. Khan, Z. Ahmad Khan (2018). Experimental and numerical investigations of nano-additives enhanced paraffin in a shell-and-tube heat exchanger: a comparative study, Applied Thermal Engineering. https://doi.org/10.1016/j.applthermaleng.2018.07.141.
[28] S.A. Marzouk a, M.M. Abou Al-Sood a, Magda K. ElFakharany a, Emad M.S. El-Said b (2020). Thermo-hydraulic study in a shell and tube heat exchanger using rod inserts consisting of wire-nails with air injection: Experimental study. International Journal of Thermal Sciences. https://doi.org/10.1016/j.ijthermalsci.2020.106742.
[29] Frank M White, Henry Xue, Fluid Mechanics, Ninth Edition, Tata McGraw hill Publication, (2022).
[30] Mohammad Reza Safarian, Farivar Fazelpour, Mehrzad Sham (2019). Numerical study of shell and tube heat exchanger with diferent cross-section tubes and combined tubes. International Journal of Energy and Environmental Engineering 10:33–46. https://doi.org/10.1007/s40095-019-0297-9.
[31] Frank P. Incropera, David P. DeWitt, Theodore L. Bergman, Adrienne S. Lavine , Incropera's Principles of Heat and Mass Transfer, Global Edition, 8th Edition, (2017).
[32] Ramachandran Thulasiram, S. Murugapoopathi, S. Surendarnath, Beemkumar Nagappan & Yuvarajan Devarajan, RSM-Based Empirical Modeling and Thermodynamic Analysis of a Solar Flat Plate Collector with Diverse Nanofluids, Process Integration and Optimization for Sustainability, 27 February 2024. https://doi.org/10.1007/s41660-024-00400-y.
[33] M.E. Nakhchi, J. Esfahani, Sensitivity analysis of a heat exchanger tube fitted with cross-cut twisted tape with alternate Axis, J. Heat Transfer 141 (2019) 041902. https://doi.org/10.1115/1.4042780.
[34] Y. He, L. Liu, P. Li, L. Ma, Experimental study on heat transfer enhancement characteristics of tube with cross hollow twisted tape inserts, Appl. Therm. Eng. 131 (2018) 743–749. https://doi.org/10.1016/j.applthermaleng.2017.12.029.
[35] Toygun Dagdevir, Veysel Ozceyhan, An experimental study on heat transfer enhancement and flow characteristics of a tube with plain, perforated and dimpled twisted tape inserts, International Journal of Thermal Sciences Volume 159, 2021, 106564. https://doi.org/10.1016/j.ijthermalsci.2020.106564.
[36] Seyedsaeed Tabatabaeikia, Hussein A. Mohammed, Nik Nazri Nik Ghazali, Behzad Shahizare, Review Article Heat Transfer Enhancement by Using Different Types of Inserts, 2015, VL - 22. https://doi.org/10.1155/2014/250354.
[37] Miftah Altwieb, Rakesh Mishra, Aliyu M. Aliyu, Krzysztof J. Kubiak, Heat Transfer Enhancement by Perforated and Louvred Fin Heat Exchangers, Energies 2022, 15(2). https://doi.org/10.3390/en15020400.
[38] A. Vaisi, R. Moosavi, K. Javaherdeh, M. V. Sheikh Zahed, M. Mohsen Soltani, Experimental examination of condensation heat transfer enhancement with different perforated tube inserts, Experimental Heat Transfer, 36(2), 183–209, 2021. https://doi.org/10.1080/08916152.2021.1991510.
[39] Rashidi, Saman & Eskandarian, Mohammad & Mahian, Omid & Poncet, Sébastien, Combination of nanofluid and inserts for heat transfer enhancement: Gaps and challenges. Journal of Thermal Analysis and Calorimetry, 2019, 135. 437-460. https://doi.org/10.1007/s10973-018-7070-9.
[40] Noor Fouad A. HamzaCorresponding Author; Sattar Aljabair, Experimental study of heat transfer enhancement using hybrid nanofluid and twisted tape insert in heat exchangers, AIP Conf. Proc. 2830, 070009, 2023. https://doi.org/10.1063/5.0163912.
[41] Fazel, M., Sadrhosseini, *H*., 2021. Entropy generation analysis in a tube heat exchanger integrated with triple blade vortex generator inserts. Energy Sources Part A: Recovery Utilization and Environmental Effects 43(1), 1–15. https://doi.org/10.1080/15567036.2021.1918291.
[42] Günes, S., Manay, E., Şenyigit, E., Özceyhan, V., 2011. A Taguchi approach for optimization of design parameters in a tube with coiled wire inserts. Appl. Therm. Eng. 31, 2568–2575. https://doi.org/10.1016/j.applthermaleng.2011.04.022.

[43] Rout, S.K., Hussein, A.K., Mohanty, C.P., 2015. Multi-objective optimization of a three-dimensional internally finned tube based on Response Surface Methodology (RSM). J. Therm. Eng. 1(2), 131–142. https://doi.org/10.18186/jte.82948.
[44] Zeng, M., Tang, L.-*H*., Lin, M., Wang, Q.-W., 2010. Optimization of heat exchangers with vortex-generator fin by Taguchi method. Appl. Therm. Eng. 30(13), 1775–1783. https://doi.org/10.1016/j.applthermaleng.2010.04.009.
[45] Chakradhar, D., Venu Gopal, A., 2011. Multi-objective optimization of electrochemical machining of EN31 steel by grey relational analysis. Int. J. Model. Optim. 1(2), 113–117. https://doi.org/10.7763/IJMO.2011.V1.20.
[46] S. Chamoli, R. Lu, D. Xu, P. Yu, Thermal performance improvement of a solar air heater fitted with winglet vortex generators, Sol. Energy 159 (2018) 966–983. https://doi.org/10.1016/j.solener.2017.11.046.
[47] A. Wijayanta, M. Aziz, K. Kariya, A. Miyara, Numerical study of heat transfer enhancement of internal flow using double-sided delta-winglet tape insert, Energies 11 (2018) 3170. https://doi.org/10.3390/en11113170.
[48] S. Chamoli, P. Yu, S. Yu, Multi-objective shape optimization of a heat exchanger tube fitted with compound inserts, Appl. Therm. Eng. 117 (2017) 708–724. https://doi.org/10.1016/j.applthermaleng.2017.02.047.
[49] S. Chamoli, R. Lu, J. Xie, P. Yu, Numerical study on flow structure and heat transferin a circular tube integrated with novel anchor shaped inserts, Appl. Therm. Eng. 135 (2018) 304–324. https://doi.org/10.1016/j.applthermaleng.2018.02.052.
[50] A. Bartwal, A. Gautam, M. Kumar, C.K. Mangrulkar, S. Chamoli, Thermal performance intensification of a circular heat exchanger tube integrated with compound circular ring–m
[51] Gurbir Singh, Hemant Kumar (2014) . Computational Fluid Dynamics Analysis of Shell and Tube Heat Exchanger. Journal of Civil Engineering and Environmental Technology, , pp. 66-70.
[52] Mohammed Irshad, Mohammed Kaushar, G. [1] A. Nouri-Borujerdi, M. Nakhchi, Friction factor and Nusselt number in annular flows with smooth and slotted surface, Heat Mass Transf. 55 (2019) 645–653. https://doi.org/10.1007/s00231-018-2445-9.
[53] M. Nakhchi, Experimental optimization of geometrical parameters on heat transfer and pressure drop inside sinusoidal wavy channels, Therm. Sci. Eng. Prog. (2018). https://doi.org/10.1016/j.tsep.2018.11.006.
[54] S. Chamoli, P. Yu, A. Kumar, Multi-response optimization of geometric and flow parameters in a heat exchanger tube with perforated disk inserts by Taguchi grey relational analysis, Appl. Therm. Eng. 103 (2016) 1339–1350. https://doi.org/10.1016/j.applthermaleng.2016.04.166.
[55] S.K. Singh, M. Kumar, A. Kumar, A. Gautam, S. Chamoli, Thermal and friction characteristics of a circular tube fitted with perforated hollow circular cylinder inserts, Appl. Therm. Eng. 130 (2018) 230–241. https://doi.org/10.1016/j.applthermaleng.2017.10.090.
[56] A.T. Wijayanta, I. Yaningsih, M. Aziz, T. Miyazaki, S. Koyama, Double-sided deltawing tape inserts to enhance convective heat transfer and fluid flow characteristics of a double-pipe heat exchanger, Appl. Therm. Eng. 145 (2018) 27–37. https://doi.org/10.1016/j.applthermaleng.2018.09.009.
[57] S. Chamoli, R. Lu, P. Yu, Thermal characteristic of a turbulent flow through a circular tube fitted with perforated vortex generator inserts, Appl. Therm. Eng. 121 (2017) 1117–1134. https://doi.org/10.1016/j.applthermaleng.2017.03.145.
[58] Manglik, R.M., Bergles, A.E., 1993. Heat transfer and pressure drop correlations for twisted-tape inserts in isothermal tubes: Part II—transition and turbulent flows. Journal of Heat Transfer 115(4), 890–896. https://doi.org/10.1115/1.2911384.